

Icc: an R package to estimate the concordance correlation, Pearson correlation, and accuracy over time

Thiago P Oliveira¹ Corresp., Equal first author, 1, 2, Rafael A Moral³ Equal first author, 3, Silvio S Zocchi⁴, Clarice GB Demetrio⁴, John Hinde¹

¹ School of Mathematics, Statistics and Applied Mathematics, NUI Galway, Galway, Ireland

² The Insight Centre for Data Analytics, NUI Galway, Galway, Ireland

³ Department of Mathematics and Statistics, National University of Ireland, Maynooth, Maynooth, Co. Kildare, Ireland

⁴ Departamento de Ciências Exatas, Luiz de Queiroz College of Agriculture - USP, Piracicaba, São Paulo, Brazil

Corresponding Author: Thiago P Oliveira
Email address: thiago.paula.oliveira@usp.br

Background and Objective: Observational studies and experiments in medicine, pharmacology, and agronomy are often concerned with assessing whether different methods/raters produce similar values over the time when measuring a quantitative variable. This paper aims to describe the statistical package *Icc*, for are, that can be used to estimate the extent of agreement between two (or more) methods over the time, and illustrate the developed methodology using three real examples.

Methods: The longitudinal concordance correlation, longitudinal Pearson correlation, and longitudinal accuracy functions can be estimated based on fixed effects and variance components of the mixed-effects regression model. Inference is made through bootstrap confidence intervals and diagnostic can be done via plots, and statistical tests.

Results: The main features of the package are estimation and inference about the extent of agreement using numerical and graphical summaries. Moreover, our approach accommodates both balanced and unbalanced experimental designs or observational studies, and allows for different within-group error structures, while allowing for the inclusion of covariates in the linear predictor to control systematic variations in the response. All examples show that our methodology is flexible and can be applied to many different data types.

Conclusions: The *Icc* package, available on the CRAN repository, proved to be a useful tool to describe the agreement between two or more methods over time, allowing the detection of changes in the extent of agreement. The inclusion of different structures for the variance-covariance matrices of random effects and residuals makes the package flexible for working with different types of databases.

1 lcc: an R package to estimate the 2 concordance correlation, Pearson 3 correlation, and accuracy over time

4 Thiago P. Oliveira^{1,2,3}, Rafael A. Moral^{3,4}, Silvio S. Zocchi⁵, Clarice G. B.
5 Demétrio⁵, and John Hinde¹

6 ¹School of Mathematics, Statistics and Applied Mathematics, NUI Galway, Galway
7 Ireland

8 ²The Insight Centre for Data Analytics, NUI Galway, Galway Ireland

9 ³Equal first author

10 ⁴Department of Mathematics and Statistics, National University of Ireland, Maynooth,
11 Maynooth, Co. Kildare, Ireland

12 ⁵Departamento de Ciências Exatas, Luiz de Queiroz College of Agriculture - USP,
13 Piracicaba, São Paulo, Brazil

14 Corresponding author:

15 Thiago Oliveira¹

16 Email address: thiago.paula.oliveira@usp.br

17 ABSTRACT

18 **Background and Objective:** Observational studies and experiments in medicine, pharmacology, and
19 agronomy are often concerned with assessing whether different methods/raters produce similar values
20 over the time when measuring a quantitative variable. This paper aims to describe the statistical package
21 `lcc`, for are, that can be used to estimate the extent of agreement between two (or more) methods over
22 the time, and illustrate the developed methodology using three real examples.

23 **Methods:** The longitudinal concordance correlation, longitudinal Pearson correlation, and longi-
24 tudinal accuracy functions can be estimated based on fixed effects and variance components of the
25 mixed-effects regression model. Inference is made through bootstrap confidence intervals and diagnostic
26 can be done via plots, and statistical tests.

27 **Results:** The main features of the package are estimation and inference about the extent of
28 agreement using numerical and graphical summaries. Moreover, our approach accommodates both
29 balanced and unbalanced experimental designs or observational studies, and allows for different
30 within-group error structures, while allowing for the inclusion of covariates in the linear predictor to control
31 systematic variations in the response. All examples show that our methodology is flexible and can be
32 applied to many different data types.

33 **Conclusions:** The `lcc` package, available on the CRAN repository, proved to be a useful tool
34 to describe the agreement between two or more methods over time, allowing the detection of changes in
35 the extent of agreement. The inclusion of different structures for the variance-covariance matrices of
36 random effects and residuals makes the package flexible for working with different types of databases.

40 INTRODUCTION

41 Agreement indices are generally used when the same experimental unit is measured by at least two
42 methods or observers (King et al., 2007). Measurements of agreement between raters or methods can be
43 used in any field to explore their interchangeability considering a certain degree of agreement between the
44 measurements they provide (Barnhart and Williamson, 2001; Chen and Barnhart, 2013). In biomedical
45 sciences it is often necessary to study the reproducibility of continuous measurements made using specific

46 diagnostic tools or methods, and that measurements can be taken over the time on the subjects of interest,
47 such as in the studies of Pandit et al. (2019); Shinar et al. (2019) and Loecher et al. (2019).

48 The concordance correlation coefficient (CCC) introduced by Lin (1989) is a statistic commonly
49 used to measure the agreement between methods when the response is continuous. Let Y_1 and Y_2 be two
50 random variables with a joint normal distribution

$$\begin{bmatrix} Y_1 \\ Y_2 \end{bmatrix} \sim N_2 \left(\begin{bmatrix} \mu_1 \\ \mu_2 \end{bmatrix}, \boldsymbol{\Sigma} = \begin{bmatrix} \sigma_1^2 & \sigma_{12} \\ \sigma_{12} & \sigma_2^2 \end{bmatrix} \right).$$

51 Here the expected value of the squared difference between Y_1 and Y_2 can be used as an agreement value.
52 However, it ranges from 0 (perfect agreement) to infinity, which makes its interpretation difficult. Lin
53 (1989) proposed standardizing this agreement index so that its values lie between -1 and $+1$:

$$\rho_{CCC} = 1 - \frac{E[(Y_1 - Y_2)^2]}{\sigma_1^2 + \sigma_2^2 + (\mu_1 - \mu_2)^2} = \frac{2\sigma_{12}}{\sigma_1^2 + \sigma_2^2 + (\mu_1 - \mu_2)^2} = \rho C_b,$$

54 where $\mu_1 = E(Y_1)$, $\mu_2 = E(Y_2)$, $\sigma_1^2 = \text{Var}(Y_1)$, $\sigma_2^2 = \text{Var}(Y_2)$, and $\sigma_{12} = \text{Cov}(Y_1, Y_2)$. This coefficient
55 takes the value -1 when there is perfect disagreement, zero when there is no agreement, and $+1$
56 when there is perfect agreement. Moreover, ρ , the Pearson correlation coefficient ($|\rho| \leq 1$), measures
57 how far each observation deviated from the best-fit line (a precision measure), and C_b , the accuracy
58 ($0 < C_b \leq 1$), measures how far the best-fit line deviates from the 45° line through the origin, defined as
59 $C_b = 2(\nu + \nu^{-1} + u^2)^{-1}$, where $\nu = \sigma_1^2/\sigma_2^2$ is a scale shift and $u = (\mu_1 - \mu_2)/\sqrt{\sigma_1\sigma_2}$ is a location shift
60 relative to the scale (Lin, 1989). Note that $C_b = 1$ indicates no deviation from the 45° line. In an attempt
61 to improve the inferential ability, Liao (2003) extended the concordance correlation coefficient by using
62 two random paired measurements to the identity line.

63 When pairs of samples (Y_{i1k}, Y_{i2k}) , for $i = 1, 2, \dots, N$ subjects and $k = 1, 2, \dots, K$ repeated measures,
64 corresponding to observations on the same subject or experimental unit over time, the use of generalized
65 multivariate analysis of variance to compute a weighted version of the CCC for repeated measurements is
66 recommended (Chinchilli et al., 1996). Moreover, this coefficient has also been expanded to assess the
67 agreement between more than two methods (King and Chinchilli, 2001).

68 When it is necessary to add extra variability sources due to within-subject measurements and/or
69 other covariates in the model, the CCC can be estimated through the variance components (VC) of a
70 mixed-effects model (Carrasco et al., 2009). The advantages of the mixed-effects models are that they
71 give a general approach to analyse repeated measures and unbalanced data; they allow for the inclusion
72 of different variance-covariance structures for both random effects and sampling errors. The restricted
73 maximum likelihood (REML) approach can be used to obtain unbiased estimates of the VC.

74 Nevertheless, sometimes the researcher is not interested in reducing the CCC for repeated measure-
75 ments to a single value, as proposed by Carrasco et al. (2009) and Carrasco et al. (2013), but in describing
76 the extent of agreement between methods over time, as discussed by Liao (2005) in a non-parametric
77 case. However, in the parametric case, we can consider a linear or non-linear function of the time and/or
78 covariates in the model to describe the response variable, as proposed by Rathnayake and Choudhary
79 (2017) and Oliveira et al. (2018). Here, we present the implementation of this methodology as an R
80 (R core Team, 2019) package `lcc` (Oliveira et al., 2019), which provides functions for estimating the
81 longitudinal concordance correlation (LCC) between methods based on variance components and fixed
82 effects using polynomial mixed-effects models. It also computes estimates for the longitudinal Pearson
83 correlation (LPC), which measures the precision, and the longitudinal bias correction factor (LA), which
84 provides an accuracy measure.

85 The `lcc()` function gives fitted values and non-parametric bootstrap confidence intervals for the
86 LCC, LPC, and LA statistics. Moreover, they can be estimated using different structures for the variance-
87 covariance matrices of the random effects and different variance functions to model heteroskedasticity of
88 within-group errors, with the option of using time as a variance covariate.

89 The remainder of the paper is organized as follows: Section introduces the theoretical definition of the
90 LCC. Section introduces the `lcc()` function input and output, describing in detail the various options as
91 well the `summary()` and other generic methods. Section briefly discusses model specification, which
92 is illustrated more extensively in Section using three real data examples. The first and third shows
93 an application in biomedical science, while the second from food science was the motivation for the

94 development of the methodology and software and nicely shows the utility of the approach. Finally,
95 Section presents some final remarks about the `lcc` package.

96 MODELS AND COMPUTATIONAL METHODS

97 Suppose a researcher is interested in investigating the extent of agreement between two or more methods,
98 indexed as $j = 1, 2, \dots, J$. Let N be the number of subjects in the experiment or observational study,
99 indexed as $i = 1, 2, \dots, N$, and suppose that each subject is observed n_i times (visits) with associated
100 nuisance factors and/or covariates, these could include, for example, the effect of block or group. Let
101 y_{ijk} be a realization of a random variable Y_{ijk} measured on the i -th subject by the j -th method at time t_k ,
102 $k = 1, 2, \dots, n_i$, with additional subject level (nuisance) covariates \mathbf{x}_i . Here t_k assumes values of the time
103 covariate $t \in \mathcal{T}$, where \mathcal{T} denotes the set of measurement times. Hence, the linear mixed-effects model
104 including a polynomial function of time per method, random effects of subject, as well random effects for
105 as subject/time interactions, is given by

$$Y_{ijk} = \boldsymbol{\gamma}^T \mathbf{x}_i + \sum_{h=0}^p \beta_{hj} t_{ik}^h + \sum_{h=0}^q b_{hi} t_{ik}^h + \boldsymbol{\varepsilon}_{ijk}, \quad (1)$$

with $\mathbf{b}_i \sim \text{MVN}(\mathbf{0}, \mathbf{G})$ and $\boldsymbol{\varepsilon}_i \sim \text{MVN}(\mathbf{0}, \mathbf{R}_i)$,

106 where $h = 1, 2, \dots, q, q+1, \dots, p$ is an index identifying the degree of the polynomial, with $q \leq p$; Y_{ijk} is
107 the response measured on the i -th subject by the j -th method at time t_{ik} ; t_{ik} represents the time (seconds,
108 minutes, days, etc) at which the i -th individual was observed; $\boldsymbol{\gamma}$ is a vector of fixed effect parameters
109 for the subject level covariates; $\boldsymbol{\beta}_j = [\beta_{0j}, \beta_{1j}, \dots, \beta_{pj}]^T$ is a $(p+1)$ -dimensional vector of fixed effects
110 for the j -th method; $\mathbf{b}_i = [b_{0i}, b_{1i}, \dots, b_{qi}]^T$ is a $(q+1)$ -dimensional vector of random effects with mean
111 vector $\mathbf{0}$ and covariance matrix \mathbf{G} ; $\boldsymbol{\varepsilon}_i$ is a $(J \times n_i)$ -dimensional error vector assumed to be independent for
112 different i and independent of the random effects, with independent entries over j and k , with mean vector
113 $\mathbf{0}$ and diagonal variance matrix \mathbf{R}_i .

114 Under model (1), the longitudinal concordance correlation (LCC) function between methods j and j' ,
115 $j \neq j'$, is given by

$$\rho_{jj'}(t_k) = \frac{\mathbf{t}_k \mathbf{G} \mathbf{t}_k^T}{\mathbf{t}_k \mathbf{G} \mathbf{t}_k^T + \frac{1}{2} \left\{ \sigma_{\varepsilon}^2 [g(t_k, \boldsymbol{\delta}_j) + g(t_k, \boldsymbol{\delta}_{j'})] + S_{jj'}^2(t_k) \right\}} = \rho_{jj'}^{(p)}(t_k) C_{jj'}(t_k) \quad (2)$$

116 where $S_{jj'}(t_k) = \mathbf{t}_k (\boldsymbol{\beta}_j - \boldsymbol{\beta}_{j'})$ is the systematic difference between methods j and j' ; $\mathbf{t}_k^T = (t_k^0, t_k^1, \dots, t_k^q)^T$;
117 $g(\cdot)$ is a variance function assumed continuous in $\boldsymbol{\delta}$; $\boldsymbol{\delta}_j$ is a vector of variance parameters for observations
118 measured by j -th method or observer. We have that $\rho_{jj'}^{(p)}(t_k)$ is the longitudinal Pearson correlation (LPC)
119 that measures how far each observation deviated from the best-fit line at a fixed time $t_k = t$, given by

$$\rho_{jj'}^{(p)}(t_k) = \frac{\mathbf{t}_k \mathbf{G} \mathbf{t}_k^T}{\sqrt{[\mathbf{t}_k \mathbf{G} \mathbf{t}_k^T + \sigma_{\varepsilon}^2 g(t_k, \boldsymbol{\delta}_j)] [\mathbf{t}_k \mathbf{G} \mathbf{t}_k^T + \sigma_{\varepsilon}^2 g(t_k, \boldsymbol{\delta}_{j'})]}}.$$

120 $C_{jj'}(t_k)$, the longitudinal accuracy (LA), measures how far the best-fit line deviates from the 45° line at a
121 fixed time $t_k = t$, given by

$$C_{jj'}(t_k) = \frac{2}{v_{jj'}(t_k) + [v_{jj'}(t_k)]^{-1} + u_{jj'}^2(t_k)},$$

122 where

$$v_{jj'}(t_k) = \sqrt{\frac{\text{Var}(Y_{ijkl})}{\text{Var}(Y_{ij'kl})}} = \sqrt{\frac{\mathbf{t}_k \mathbf{G} \mathbf{t}_k^T + \sigma_{\varepsilon}^2 g(t_k, \boldsymbol{\delta}_j)}{\mathbf{t}_k \mathbf{G} \mathbf{t}_k^T + \sigma_{\varepsilon}^2 g(t_k, \boldsymbol{\delta}_{j'})}}$$

123 denotes the scale shift at time $t_k = t$, and

$$u_{jj'}(t_k) = \frac{E(Y_{ijkl}) - E(Y_{ij'kl})}{[\text{Var}(Y_{ijkl}) \text{Var}(Y_{ij'kl})]^{\frac{1}{4}}} \\ = \frac{t_k(\boldsymbol{\beta}_j - \boldsymbol{\beta}_{j'})}{\{[t_k \mathbf{G}t_k^T + \sigma_{\epsilon}^2 g(t_k, \boldsymbol{\delta}_j)] [t_k \mathbf{G}t_k^T + \sigma_{\epsilon}^2 g(t_k, \boldsymbol{\delta}_{j'})]\}^{\frac{1}{4}}}$$

124 denotes the location shift at time t_k relative to the scale (Lin, 1989; Oliveira et al., 2018). Consequently,
125 when $\text{Var}(Y_{ijkl}) = \text{Var}(Y_{ij'kl})$ and $E(Y_{ijkl}) = E(Y_{ij'kl})$ then $C_{jj'}(t_k) = 1$ and there is no deviation from
126 the 45° line.

127 Estimation and Inference

128 Point estimation and statistical inference for the LCC ($\rho_{jj'}(t_k)$) has been proposed by Oliveira et al.
129 (2018). It is estimated by replacing $\boldsymbol{\beta}$ and the variance components by their respective REML estimates:

$$\hat{\rho}_{jj'}(t_k) = \frac{t_k \hat{\mathbf{G}}t_k^T}{t_k \hat{\mathbf{G}}t_k^T + \frac{1}{2} \left\{ \hat{\sigma}_{\epsilon}^2 \left[\hat{g}(t_k, \hat{\boldsymbol{\delta}}_j) + \hat{g}(t_k, \hat{\boldsymbol{\delta}}_{j'}) \right] + \hat{S}_{jj'}^2(t_k) \right\}}.$$

130 Since the variance components are estimated using the REML approach, their estimates are asymp-
131 totically normally distributed and the bias is smaller when compared to the maximum likelihood (ML)
132 approach. Moreover, Oliveira et al. (2018) showed a satisfactory performance of the LCC even in settings
133 with severe imbalance and only a small number of subjects ($N = 20$).

134 A confidence interval (CI) for $\rho_{jj'}(t_k)$ can be constructed using a nonparametric bootstrap based on M
135 (e.g. 5000) bootstrap samples with either the percentile method (recommended for $N \leq 30$) or, otherwise,
136 a normal approximation confidence interval, as described by Oliveira et al. (2018).

When we use a normal approximation for the CI, the Fisher Z-transformation given by

$$\rho_{j,j'}^*(t_k) = \frac{1}{2} \ln \left[\frac{1 + \rho_{j,j'}(t_k)}{1 - \rho_{j,j'}(t_k)} \right]$$

should be used with the normal approximation made to the empirical distribution of $\rho_{j,j'}^*(t_k)$ (Lin, 1989).
Consequently, the confidence limits can be estimated using the bootstrap estimator of $\rho_{j,j'}^*(t_k)$ for a fixed
time $t_k = t$ given by

$$\hat{\rho}_{j,j'}^*(t_k = t) = \frac{1}{2M} \sum_{m=1}^M \ln \left[\frac{1 + \hat{\rho}_{j,j'}^{(m)}(t)}{1 - \hat{\rho}_{j,j'}^{(m)}(t)} \right], \quad m = 1, 2, \dots, M,$$

where $\{\hat{\rho}_{j,j'}^{(m)}\}$ are the estimates from the M bootstrap samples. The standard deviation of the bootstrap
distribution of $\hat{\rho}_{j,j'}^*(t_k)$ for a fixed time $t_k = t$ given by

$$\widehat{SE}_{j,j'}^*(t_k = t) = \sqrt{\frac{1}{M-1} \sum_{m=1}^M \left[\frac{1}{2} \ln \left(\frac{1 + \hat{\rho}_{j,j'}^{(m)}(t)}{1 - \hat{\rho}_{j,j'}^{(m)}(t)} \right) - \hat{\rho}_{j,j'}^*(t) \right]^2}.$$

137 Thus, an approximate bootstrap confidence interval of level $(1 - \alpha)$ for $\rho_{j,j'}$ is $[LB, UB]$, where

$$LB = \frac{\exp \left\{ 2 \left[\hat{\rho}_{j,j'}^*(t_k = t) - z_{(1-\frac{\alpha}{2})} \widehat{SE}_{j,j'}^*(t_k = t) \right] \right\} - 1}{\exp \left\{ 2 \left[\hat{\rho}_{j,j'}^*(t_k = t) - z_{(1-\frac{\alpha}{2})} \widehat{SE}_{j,j'}^*(t_k = t) \right] \right\} + 1}$$

138 and

$$UB = \frac{\exp \left\{ 2 \left[\hat{\rho}_{j,j'}^*(t_k = t) + z_{\frac{\alpha}{2}} \widehat{SE}_{j,j'}^*(t_k = t) \right] \right\} - 1}{\exp \left\{ 2 \left[\hat{\rho}_{j,j'}^*(t_k = t) + z_{\frac{\alpha}{2}} \widehat{SE}_{j,j'}^*(t_k = t) \right] \right\} + 1},$$

139 where $z_{\frac{\alpha}{2}}$ and $z_{(1-\frac{\alpha}{2})}$ denote the $\frac{\alpha}{2}$ and $(1-\frac{\alpha}{2})$ percentiles of the standard normal distribution.

On the other hand, the CI based on the percentile method uses the percentiles of the bootstrap distribution of $\hat{\rho}_{j,j'}(t_k = t)$ directly and is given by

$$\left(\hat{\rho}_{j,j'}^{(\alpha/2)}(t_k = t), \hat{\rho}_{j,j'}^{(1-\alpha/2)}(t_k = t)\right) \approx \left(\hat{\rho}_{j,j'}^{(m)(\alpha/2)}(t_k = t), \hat{\rho}_{j,j'}^{(m)(1-\alpha/2)}(t_k = t)\right),$$

140 where $\hat{\rho}_{j,j'}^{(m)(\alpha/2)}(t_k = t)$ and $\hat{\rho}_{j,j'}^{(m)(1-\alpha/2)}(t_k = t)$ are the $(100 \times \frac{\alpha}{2})$ -th and $(100 \times 1 - \frac{\alpha}{2})$ -th empirical
141 percentiles of the $\hat{\rho}_{j,j'}^{(m)}(t_k = t)$ values, $m = 1, 2, \dots, M$. If the bootstrap distribution of $\rho_{j,j'}^*(t_k = t)$ is
142 approximately normal, then both proposed methods will give very similar confidence intervals as N
143 increases.

Inference for $C_{j,j'}(t_k)$ can be performed in a similar way as to that presented for the LCC. Since $C_{(j,j')(1-\alpha/2)}(t_k = t)$ belongs to the interval $[0, 1]$, we suggest the use the arc-sine transformation

$$C_{(j,j')(1-\alpha/2)}^*(t_k = t) = \sin^{-1} \sqrt{C_{j,j'}(t_k)}$$

instead of the Fisher Z-transformation, nor logistic transformation (used by Oliveira et al. (2018)) to approximate the distribution of $C_{(j,j')(1-\alpha/2)}(t_k = t)$ by a normal distribution. Thus, the confidence limits can be estimated using the bootstrap estimator of $C_{j,j'}^*(t_k)$ for a fixed time $t_k = t$ given by

$$\hat{C}_{j,j'}^*(t_k = t) = \frac{1}{M} \sum_{m=1}^M \sin^{-1} \sqrt{\hat{C}_{j,j'}^{(m)}(t)}, \quad m = 1, 2, \dots, M,$$

and standard deviation of the bootstrap distribution of $\hat{C}_{j,j'}^*(t_k)$ for a fixed time $t_k = t$ is given by

$$\widehat{SE}_{C_{j,j'}^*}(t_k = t) = \sqrt{\frac{1}{M-1} \sum_{m=1}^M \left[\sin^{-1} \sqrt{\hat{C}_{j,j'}^{(m)}(t)} - \hat{C}_{j,j'}^*(t) \right]^2}.$$

144 Therefore, an approximate bootstrap confidence interval of level $(1-\alpha)$ for $\hat{C}_{j,j'}$ is $[LB_C, UB_C]$, where

$$LB_C = \text{sign} \left[\hat{C}_{j,j'}^*(t_k = t) - z_{(1-\frac{\alpha}{2})} \widehat{SE}_{C_{j,j'}^*}(t_k = t) \right] \left\{ \sin \left[\hat{C}_{j,j'}^*(t_k = t) - z_{(1-\frac{\alpha}{2})} \widehat{SE}_{C_{j,j'}^*}(t_k = t) \right] \right\}^2$$

145 and

$$UB_C = \text{sign} \left[\hat{C}_{j,j'}^*(t_k = t) - z_{\frac{\alpha}{2}} \widehat{SE}_{C_{j,j'}^*}(t_k = t) \right] \left\{ \sin \left[\hat{C}_{j,j'}^*(t_k = t) - z_{\frac{\alpha}{2}} \widehat{SE}_{C_{j,j'}^*}(t_k = t) \right] \right\}^2,$$

146 where $z_{\frac{\alpha}{2}}$ and $z_{(1-\frac{\alpha}{2})}$ denote the $(\frac{\alpha}{2})$ and $(1-\frac{\alpha}{2})$ quantiles of the standard normal distribution. Bootstrap
147 percentile intervals are calculated in the obvious way from the bootstrap values $\hat{C}_{j,j'}^{(m)}(t)$, $m = 1, 2, \dots, M$.

148 OVERVIEW OF THE PACKAGE `lcc` AND R SYNTAX

149 This section provides some details on the implementation of the function `lcc` and explains its technical
150 arguments, whose default settings were carefully chosen. The package is freely available for download
151 from the CRAN website <https://CRAN.R-project.org/package=lcc>, and installation can be performed
152 using

```
153 R> install.packages("lcc")
154 R> library(lcc)
```

155 The `lcc` package has 21 arguments that are briefly summarised in Table 1.

Table 1. Input arguments for LCC package

Argument	Type	Description	Default	Required
<code>data</code>	<code>data.frame</code>	Specifies the input dataset		Yes
<code>resp</code>	Character string	Name of the response variable		Yes
<code>subject</code>	Character string	Name of the subject variable		Yes
<code>method</code>	Character string	Name of the method variable		Yes
<code>time</code>	Character string	Name of the time variable		Yes
<code>interaction</code>	Logical	an option to estimate the interaction effects between method and time. If TRUE the interaction effects are estimated. If FALSE only the main effects of time and method are estimated	TRUE	No
<code>qf</code>	Numeric	An integer specifying the degree of the polynomial time trends, usually 1, 2 or 3 (0 is not allowed).	1	No
<code>qr</code>	Numeric	An integer specifying terms having random effects to account for subject-to-subject variation, such that $qr \leq qf$, and $qr=0$ means there is just a random intercept.	0	No
<code>covar</code>	Character vector	Names of the covariates (factors and/or variables) to include in the model as fixed effects, e.g. block, group, etc.	NULL	No
<code>gs</code>	Character string	Name of method level which represents the gold-standard.	first level	No
<code>pdmat</code>	Function	Standard classes of positive-definite matrix structures available in the nlme package.	pdSymm	No
<code>var.class</code>	Function	Standard classes of variance function structures used to model the variance structure of within-group errors using covariates.	NULL	No
<code>weights.form</code>	Formula	An one-sided formula specifying a variance covariate and, optionally, a grouping factor for the variance parameters in the <code>var.class</code> . If <code>var.class = varIdent</code> , the form "method", (or $\sim 1 \text{method}$), or "time.ident" ($\sim 1 \text{time}$), must be used. If <code>var.class = varExp</code> , the form "time" ($\sim \text{time}$), or "both" ($\sim \text{time} \text{method}$), must be used.	NULL	No ¹

Continued on next page

¹Required when `var.class` is specified.

Table 1 – continued from previous page

Argument	Type	Description	Default	Required
<code>time.lcc</code>	List	Regular sequence for time variable merged with specific or experimental time values used for LCC, LPC, and LA predictions.	NULL	No
<code>ci</code>	Logical	An optional non-parametric bootstrap confidence interval for the LCC, LPC and LA statistics. If TRUE confidence intervals are calculated and printed in the output.	FALSE	No
<code>percentileMet</code>	Logical	an optional method for calculating the non-parametric bootstrap intervals. If FALSE the normal approximation method is used. If TRUE the percentile method is used.	FALSE	No ²
<code>alpha</code>	Numeric	Confidence level for the CI.	0.05	No ²
<code>nboot</code>	Numeric	An integer specifying the number of bootstrap samples.	5000	No ²
<code>show.warnings</code>	Logical	an optional argument that shows the number of convergence errors in the bootstrap samples. If TRUE shows in which bootstrap samples the errors occurred. If FALSE shows the total number of convergence errors.	FALSE	No
<code>components</code>	Logical	An option to estimate the LPC and LA statistics. If TRUE the estimates and confidence intervals for LPC and LA are printed in the output. If FALSE provides estimates and confidence intervals only for the LCC statistic.	FALSE	No
<code>REML</code>	Logical	The estimation method. If TRUE the model is fit by maximizing the restricted log-likelihood. If FALSE full maximum likelihood is used.	TRUE	No
<code>lme.control</code>	List	A list of control values passed to the estimation algorithm to replace the default values of the function <code>lmeControl</code> available in the <code>nlme</code> package.	empty list	No
<code>numCore</code>	Integer	Number of cores used in parallel during bootstrapping computation	1	No

156 We present a more detailed description of some arguments below:

- 157 1. `data`: must be a data frame containing the following variables: response, subject identification,
158 method, and time;
- 159 2. `method`: name of the method variable in the dataset. The `lcc` package recognizes the first level
160 of the variable associated with this argument as the gold-standard method, and then compares it
161 with all other levels;
- 162 3. `qr`: when we specify $qr = 0$ a random intercept is included in the polynomial model while qr
163 $= 1$ specifies random intercepts and slopes. If $qr = qf = q$, with $q \geq 1$, all polynomial terms

²It can only be specified when `ci = TRUE`

164 are specified to have random effects at the individual level.

165 4. `time_lcc`: a named list with values for arguments `time`, `from`, `to`, and `n` used in the `time_lcc()`
 166 function to generate a regular sequence merged with specific or experimental time values of the
 167 time variable used for LCC, LPC and LA predictions. Argument `time` is a vector of specific or
 168 experimental time values of a given length, where the experimental time values are used as default;
 169 `from` and `to` are used to define, respectively, the starting and end values of the time variable, and
 170 `n` is used to define the desired length of the sequence. We recommend a grid $\mathbf{t} = (t_1, t_2, \dots, t_{n^*})^T$ of
 171 n^* points in \mathcal{T} to construct the agreement curve and confidence intervals. In practice, n^* between
 172 30 and 50 is generally adequate. Example:

```
173 R> Time <- seq(0, 20, 1)
174 R> str(tk <- time_lcc(time=Time, from=min(Time), to=max(Time),
175 + n=30))
176 num [1:49] 0 0.69 1 1.38 2 ...
```

177 5. `pdmat`: the `lcc` package provides six standard classes of positive-definite matrix structures that
 178 can be included in the model to estimate the LCC, LPC and LA statistics. Available standard
 179 classes are `pdSymm`, `pdLogChol`, `pdDiag`, `pdIdent`, `pdCompSymm`, and `pdNatural`. More
 180 information about these classes are available in Pinheiro and Bates (2000).

181 6. `var.class`: a class of variance functions that are used to model the variance structure of within-
 182 group errors using covariates (Pinheiro and Bates, 2000). We generalize this class as

$$\text{Var}(\varepsilon_{ijk}) = \sigma_{\varepsilon}^2 g(t_k, \boldsymbol{\delta}), \quad (3)$$

183 where $g(\cdot)$ is the variance function assumed continuous in $\boldsymbol{\delta}$; t_k is the time covariate and $\boldsymbol{\delta}$ is a
 184 vector of variance parameters. The `lcc` package provides two different standard variance functions
 185 classes that are included in the `nlme` library (Pinheiro et al., 2017).

186 The first one is the `varIdent` class that represent a variance model with different variances for
 187 each level of a stratification variable s , $s = 1, 2, \dots, S$, given by

$$\text{Var}(\varepsilon_{ijk}) = \sigma_{\varepsilon}^2 \delta_{s_{ijk}}^2.$$

188 As we have $S + 1$ parameters to represent S variances, we need to add the restriction $\delta_1 = 1$, and
 189 consequently $\delta_{s^*} = \delta_{s^*} / \delta_1$, $s^* = 2, 3, \dots, S$ and $\delta_{s^*} > 0$. Here each level of method/observer or time
 190 represents a stratum of a homogeneous subgroup.

191 The second variance function is an exponential function of the variance covariate, the `varExp`
 192 class, represented as

$$\text{Var}(\varepsilon_{ijk}) = \sigma_{\varepsilon}^2 \exp(2\delta_{s_{ijk}} t_k)$$

193 where $\delta_{s_{ijk}}$ is unrestricted, so the variance model (4) allows $\text{Var}(\varepsilon_{ijk})$ to increase or decrease over
 194 time.

195 7. `weights.form`: a `varFunc` class object, representing a constructor to the `form` argument in
 196 the `nlme` library. The `weights.form` argument is based on a one-sided formula specifying a
 197 variance covariate and, optionally, a grouping factor for the variance parameters. Moreover, this
 198 argument must be specified only when `var.class` is specified as well.

199 The first class `varIdent` represents a variance model with different variances for each level of
 200 the grouping factor and has two options of `weights.form` in the `lcc` package:

201 (a) "method": specifies a variance model with different variances for each level of factor
 202 method/observer and is given by

$$\text{Var}(\varepsilon_{ijk}) = \sigma_{\varepsilon}^2 \delta_{\text{method},j}^2, \quad j = 1, 2, \dots, J,$$

203 where $g(\text{method}_j, \delta_j) = \delta_{\text{method}_j}^2$ is the variance function, and δ_{method_j} is the variance param-
 204 eter for observations measured by the j th method. The `form` argument in the `varFunc` is
 205 `form = ~ 1|method`;

206 (b) `"time.ident"`: specifies a variance model with different variances for each level of
 207 stratification in the time variable and is given by

$$\text{Var}(\varepsilon_{ijk}) = \sigma_\varepsilon^2 \delta_{t_k}^2, \quad k = 1, 2, \dots, K,$$

208 where $g(t_k, \delta_k) = \delta_k^2$ is the variance function, and δ_k is the variance parameter for obser-
 209 vations measured at time $t_k = t$, with $t \in [t_0, t_K]$ and $t_0 \geq 0$. The `form` argument in the
 210 `varFunc` class is `form = ~ 1|time`.

211 The class `varExp` represents a variance model whose variance function $g(\cdot)$ is an exponential
 212 function of the variance covariate. This class has also two options of `weights.form` in the `lcc`
 213 package:

214 (a) `"time"`: specifies a variance model given by

$$\text{Var}(\varepsilon_{ijk}) = \sigma_\varepsilon^2 \exp(2\delta t_k),$$

215 where the variance function $g(t_k, \delta) = \exp(2\delta t_k)$ is an exponential function of the time $t_k = t$;
 216 and δ is the variance parameter. The `form` argument in the `varFunc` class is `form = ~`
 217 `time`;

218 (b) `"both"`: specify a variance model for each level of the factor method given by

$$\text{Var}(\varepsilon_{ijk}) = \sigma_\varepsilon^2 \exp\left(2\delta_{\text{method}_j} t_k\right), \quad j = 1, 2, \dots, J,$$

219 where the variance function $g(t_k, \text{method}_j, \delta) = \exp\left(2\delta_{\text{method}_j} t_k\right)$ is an exponential function
 220 of the time $t_k = t$ for each level of method; and δ_{method_j} is the variance parameter for the j th
 221 level of method. The `form` argument in the `varFunc` class is `form = ~ time|method`;

222 The `lcc` package uses the REML method as default because it is less biased, less sensitive to outliers,
 223 and deals more effectively with high correlations when compared to standard ML estimation (Harville,
 224 1977; Giesbrecht and Burns, 1985). However, we offer the user the possibility to change the estimation
 225 method to ML because this approach should be used when comparing models with nested fixed effects but
 226 with the same random effects structure. Furthermore, the package depends on the `nlme` (Pinheiro et al.,
 227 2017), and `ggplot2` (Wickham, 2009) packages, and imports some functions from packages `gdata`
 228 (Warnes et al., 2017), `gridExtra` (Auguie and Antonov, 2017), and `hnp` (Moral et al., 2017).

229 Generic functions and outputs

230 A typical call of the `lcc` function is similar to a call to `lme` as the LCC estimation is based on a
 231 mixed-effects regression model. Several variations in the specifications of linear mixed-effects models to
 232 estimate the LCC are possible, and we can query the fitted `lcc` object through different generic functions.
 233 Table 2 gives details of a set of S3 generic extractor functions for objects of class `lcc`.

234 The output of the `summary()` function includes the values of Akaike Information Criterion (AIC)
 235 (Akaike, 1974), the Bayesian Information Criterion (BIC) (Schwarz, 1978), log-likelihood value, and a
 236 goodness of fit measurement `gof`, which is calculated using the concordance correlation coefficient (Lin,
 237 1989) between fitted values extracted from the mixed-effects model and observed values. This measure
 238 can be used, with care, to describe the overall agreement between observed and fitted values, where a
 239 value equal to -1 represents a perfect disagreement between them, zero represents no agreement, and
 240 $+1$ perfect agreement. Clearly, a high model performance is related with a high positive value of `gof`
 241 (generally between 0.8-1).

242 The fitted curves of LCC, LPC, or LA values versus the time covariate, as well as their boot-
 243 strap confidence intervals, can be visualised through the `lccPlot()` function, which is specified as

Table 2. Generic functions for use with objects of class `lcc`

Function	Description
<code>print()</code>	a simple printed display
<code>summary()</code>	returns an object of class <code>summary.lcc</code> containing the relevant summary statistics (which has a <code>print()</code> method). If <code>type = "lcc"</code> it provides information about $\rho_{jj'}(t_k)$, and if <code>components = TRUE</code> in the <code>lcc()</code> function, also provides information about $\rho_{jj'}^{(p)}(t_k)$, and $C_{jj'}(t_k)$. If <code>type = "model"</code> it provides additional information about the linear mixed-effects fit. The default is <code>type = "model"</code> .
<code>anova()</code>	Summarise and compare likelihoods of fitted models from <code>lcc</code> objects
<code>coef()</code>	The fixed effects estimated and corresponding random effects estimates are obtained at subject levels less or equal to N . The resulting estimates are returned as a data frame, with rows corresponding to subject levels and columns as coefficients.
<code>fitted()</code>	Fitted values for $\hat{\rho}_{jj'}(t_k)$, $\hat{\rho}_{jj'}^{(p)}(t_k)$, or $\hat{C}_{jj'}(t_k)$. The output depends on the argument <code>type</code> , where <code>type = "lcc"</code> (the default), <code>type = "lpc"</code> , or <code>type = "la"</code> gives output for $\hat{\rho}_{jj'}(t_k)$, $\hat{\rho}_{jj'}^{(p)}(t_k)$, or $\hat{C}_{jj'}(t_k)$, respectively.
<code>getVarCov()</code>	Returns the variance components estimates.
<code>residuals()</code>	Extract residuals (response, Pearson, and normalized), defaulting to Pearson residuals
<code>raneff()</code>	Extract the estimated random effects.
<code>vcov()</code>	Returns the variance-covariance matrix of the fixed effects.
<code>AIC()</code>	Compute the Akaike criterion
<code>BIC()</code>	Compute the Bayesian criterion
<code>logLik()</code>	Extract the log-likelihood
<code>plot()</code>	A series of six built-in diagnostic plots to evaluate the assumptions underlying the linear mixed-effects regression model. Comprises: a plot of conditional residuals against fitted values; plot of conditional residuals over time; box-plot of residuals given subject; observed against fitted values; normal Q-Q plot with simulation envelopes for the conditional errors; and normal Q-Q plot with simulation envelopes for the random effects are provided.

244 `lccPlot(obj, type, control)`, where `obj` is an object of class `lcc`; `type` specifies required
 245 output that could be `type="lcc"` for the LCC, the default, `type="lpc"` for the LPC, or `type="la"`
 246 for the LA statistics; and `control` is a list of control values or character strings returned by the
 247 `plotControl()` function used to modify the plot structure. This function uses the `ggplot2` package
 248 internally to build the final plot, where predicted values are joined by lines, sampled observations are
 249 represented by circles, and confidence intervals by a ribbon (grey as default) defined by its lower and
 250 upper bounds.

251 SPECIFYING MODELS IN THE `lcc()` FUNCTION

252 In the `lcc` package, to describe the LCC we need to specify the subject, response, method and time
 253 variables, a polynomial mixed-effect model, and the data. These arguments are specified through an
 254 easy-to-use syntax. Consider a first degree polynomial model with random intercepts for a continuous
 255 dependent variable y observed on N subjects ($i = 1, 2, \dots, N$) using J methods at times t_k ($k = 1, 2, \dots, n_i$).
 256 Such model can be written as

$$Y_{ijk} = \beta_{0j} + b_{0i} + \beta_{1j}t_k + \varepsilon_{ijk}, \text{ with} \\ b_{0i} \sim N(0, \sigma_{b_0}^2) \text{ and } \varepsilon_{ijk} \sim N(0, \sigma_{\varepsilon}^2)$$

257 Thus, the LCC based on fixed effects and variance components at time t_k is given by

$$\rho_{jj'}(t_k) = \frac{\sigma_{b_0}^2}{\sigma_{b_0}^2 + \sigma_{\varepsilon}^2 + \frac{1}{2}[\beta_{01} - \beta_{02} + (\beta_{11} - \beta_{12})t_k]^2}$$

258 and the syntax to specify this model in the `lcc()` function is

```
259 R> library(lcc)
260 R> data(simulated_hue_block)
261 R> m1 <- lcc(data = simulated_hue_block, subject = "Fruit",
262 +           resp = "Hue", method = "Method", time = "Time",
263 +           qf = 1, qr = 0)
```

264 where `qf = 1` represents the polynomial degree for the fixed effects, and `qr = 0` specifies a random intercepts model. Here, the names of the columns in the dataframe `data` are supplied as strings to the arguments of the `lcc()` function.

267 Suppose now that the experimental design in the previous example was a randomized complete block design. Then, the fixed effect of blocks can be included in that model by specifying the `covar` argument, i.e.

```
270 R> m2 <- update(m1, covar = "Block")
```

271 If we suppose different variances for each level of the method factor, the corresponding model would include a variance function such as $g(\delta_j) = \sigma_\epsilon^2 \delta_j^2$, and the syntax would then be

```
273 R> m3 <- update(m2, var.class = varIdent, weights.form = "method",
274 +           lme.control = list(opt="optim"))
```

275 To visualize the summary and graphical output of model `m3` we call `summary(m3)` and `lccPlot(m3)`, respectively.

277 Many other possible models can be built to estimate the LCC through the function `lcc()` options, see Section . Model selection can be performed using likelihood-ratio tests for nested models; or using the AIC or BIC criteria, e.g.

```
280 R> AIC(m2, m3); BIC(m2, m3); anova(m2, m3)
```

281 EXAMPLES

282 We will now use three example datasets, drawn from Lloyd et al. (1998), Martin et al. (2002) and Oliveira et al. (2018), to illustrate the implemented functions in the following sections of this paper. The first dataset is an observational study of a cohort of 82 adolescent females to assess the percentage body fat and the aim is to determine the agreement profile between measurements made over time using a skinfold caliper and dual-energy X-ray absorptiometry. The second is a canonical example from agriculture and was the motivation for the original development of these methods; here the goal is to investigate if a colorimeter can compete with a digital scanner in measuring the peel hue of papayas over time. The final example is again related to medicine and the goal here is to verify the agreement between cortisol concentration measured on patients every hour and every two hours.

291 Percentage body fat dataset

292 These data came from a longitudinal observational study conducted as part of the Penn State Young Women's Health Study (Lloyd et al., 1998). Percentage body fat was measured using skinfold calipers and dual-energy X-ray absorptiometry (DEXA) on a cohort of 82 adolescent white females attending public schools in Pennsylvania. The initial visit occurred at age 12 (baseline) and subsequent visits occurred every six months, in which one skinfold caliper and one DEXA measurement were taken to assess the percentage of body fat. As the skinfold measurement is the most frequently used method for laboratory and field studies, the objective was to determine the agreement profile between the skinfold caliper and DEXA measurements. Figure 1 shows that the agreement between skinfold and DEXA apparently decreases over the visits. King et al. (2007) explained that this phenomenon may occur because the skinfold method is only capable of detecting subcutaneous fat, while DEXA detects subcutaneous, breast, lower body and visceral fat. Moreover, female adolescents may have a considerable fat increase in breast, lower body and/or visceral fat over this age range (King et al., 2007). Consequently, this reinforces the interest in estimating the agreement profile between these methods for the body fat measurements over ages ranging from 12.5 to 13.5 years old, rather than summarizing it in a single coefficient as proposed

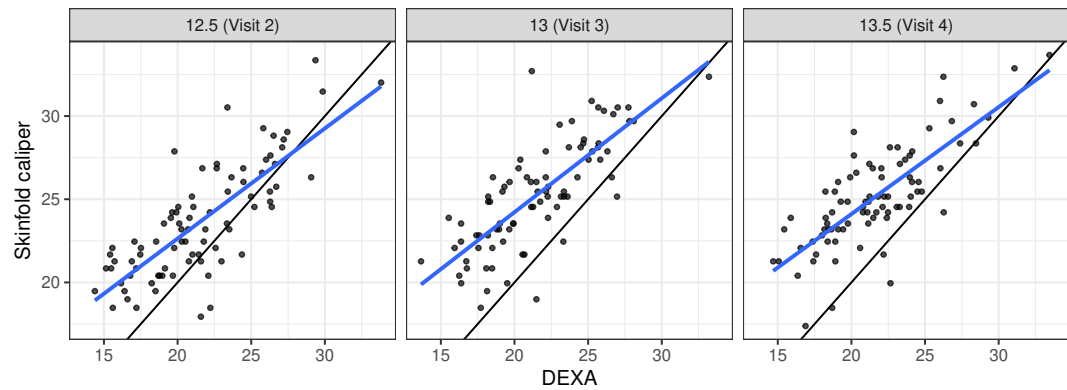


Figure 1. Scatter plot of body fat data, where the panels represent visits, the blue line is the best fit line, and the black line is the line of equality.

306 by King et al. (2007). Hence, we created a new variable called `TIME` given by $12 \times (\text{age} - 12)$, which
 307 represents the time in months after the first visit (baseline).

Now let y_{ijk} be the measurement taken on the i -th individual, by the j -th method at the k -th visit. We then fit a random intercepts and slopes linear regression model, given by

$$y_{ijk} = \beta_{0j} + b_{0i} + (\beta_{1j} + b_{1i})t_k + \varepsilon_{ijk} \quad (4)$$

$$\mathbf{b} = [b_{0i}, b_{1i}]^T \sim N_2(\mathbf{0}, \mathbf{G}) \quad \text{and} \quad \varepsilon_{ijk} \sim N(0, \sigma_\varepsilon^2),$$

308 where $\text{vech}(\mathbf{G}) = [\sigma_{b_0}^2, \sigma_{b_{01}}, \sigma_{b_1}^2]^T$ ($\text{vech}(\cdot)$ is the half-vectorization of a symmetric matrix \mathbf{G} formed
 309 from only the lower triangular part). Using model (4), we estimate the LCC, LPC and LA statistics as well
 310 as their 95% bootstrap confidence intervals based on 10,000 pseudo-samples using the `lcc()` function:

```

311 R> data(bfat, package = "cccrm")
312 R> library(dplyr)
313 R> bfat <- bfat %>%
314 +   mutate(VISITNO = replace(VISITNO, VISITNO == 2, 12.5)) %>%
315 +   mutate(VISITNO = replace(VISITNO, VISITNO == 3, 13)) %>%
316 +   mutate(VISITNO = replace(VISITNO, VISITNO == 4, 13.5)) %>%
317 +   mutate(SUBJECT = factor(SUBJECT)) %>%
318 +   mutate(MET = factor(MET, labels = c("1 hour", "2 hours")))
319 R> bfat$TIME <- 12 * (bfat$VISITNO - 12)
320 R> set.seed(134)
321 R> m.bfat.1 <- lcc(data = bfat, subject = "SUBJECT", resp = "BF",
322 +   method = "MET", time = "TIME", qf = 1, qr = 1,
323 +   components = TRUE, ci = TRUE, nboot = 10000)
324 Convergence error in 902 out of 10000 bootstrap samples.
```

325 The output of model `m.bfat.1` indicates that in 902 (9.02%) of the pseudo-samples, the likelihood
 326 maximization algorithm failed to converge, where most of these failures were a consequence of specific
 327 bootstrap sample patterns. An alternative procedure to decrease the percentage of convergence failures
 328 is by increasing the iteration limit and/or changing the optimization method from `nlminb` to `optim`.
 329 In the `lcc()` function, the user can include a list of optimisation control additional arguments in the
 330 `lme.control()` function:

```

331 R> set.seed(134)
332 R> m.bfat.2 <- update(m.bfat.1, lme.control = list(opt = "optim"))
333 Convergence error in 76 out of 10000 bootstrap samples.
```

334 The output of `m.bfat.2` shows a lower number of failures (0.76%) compared with the previous
 335 approach. We proceed to examine the bootstrap confidence intervals computed for the LCC, LPC and LA:

```

336 R> summary(m.bfat.2, type = "lcc")
337 Longitudinal concordance correlation model fit by REML
338 AIC      BIC      logLik
339 2182.068  2215.59  -1083.034
340
341 gof: 0.9201
342
343 Lower and upper bound of % bootstrap confidence interval
344 Number of bootstrap samples:
345
346 DEXA vs. skinfold
347 $LCC
348      Time      LCC      Lower      Upper
349 1      6      0.6653516  0.5687779  0.7395459
350 2     12      0.5589258  0.4516374  0.6442955
351 3     18      0.4588008  0.3353932  0.5599172
352
353 $LPC
354      Time      LPC      Lower      Upper
355 1      6      0.8065578  0.7415331  0.8558988
356 2     12      0.7826493  0.7092871  0.8378992
357 3     18      0.7620551  0.6676806  0.8300397
358
359 $LA
360      Time      LA      Lower      Upper
361 1      6      0.8249273  0.7431156  0.8898124
362 2     12      0.7141458  0.6201347  0.7923521
363 3     18      0.6020573  0.4934167  0.6961643

```

364 We may then plot the LCC, LPC, and LA with their respective confidence intervals by executing

```

365 R> lccPlot(m.bfat.2)
366 R> lccPlot(m.bfat.2, type = "lpc")
367 R> lccPlot(m.bfat.2, type = "la")

```

368 The estimates of LCC, LPC and LA, their confidence intervals, and figures indicate that the agreement
369 and accuracy profiles between the skinfold caliper and DEXA measurements decrease over time, while
370 the precision profile, represented by LPC, remains constant (Figure 2). Therefore, a first conclusion is
371 that the agreement profile decreases over time because the accuracy is decreasing.

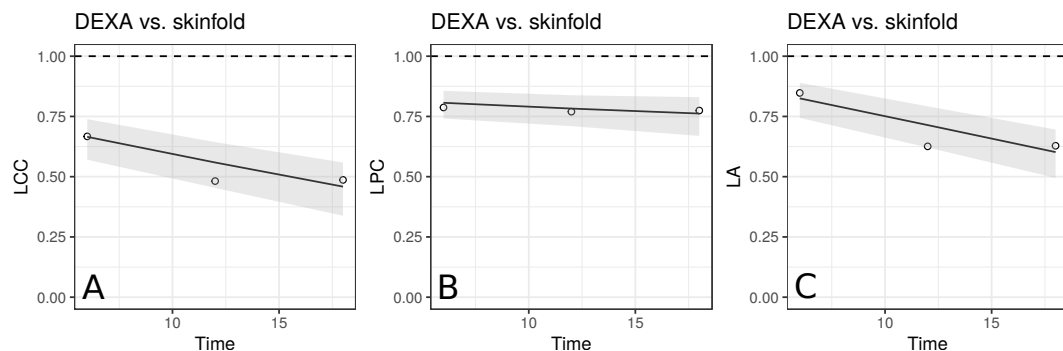


Figure 2. Estimate and 95% bootstrap confidence interval for the (A) longitudinal concordance correlation (LCC); (B) longitudinal Pearson correlation (LPC); and (C) longitudinal accuracy (LA) between percentage body fat measured on adolescent girls by skinfold caliper and DEXA. Points represent (A) the sample CCC, (B) sample Pearson correlation, and (C) sample accuracy.

Moreover, there is a moderate to weak agreement profile, where the greatest LCC estimate was 0.6654 at age 12.5 (95% CI: [0.5688, 0.7395]) and the smallest LCC estimate was 0.4588 at age 13.5 (95% CI: [0.3354, 0.5599]). This result reinforces the discussion presented by King et al. (2007), who provided physiological explanations for this phenomenon due to fact that the skinfold method is not capable to detect breast, lower body and visceral fat, which increases over this age range. Clearly, as the skinfold method detects less fat than the other, the accuracy between them tends to decrease since the expected value difference is greater (Figure 2C). The concordance correlation coefficient between fitted values of the mixed-effects model and observed values is presented as goodness of fit ($g \circ f$) and was approximately 0.92. This result shows that the model can reproduce the observed values quite well.

381 The papaya peel hue dataset

382 In commercial fruit classification, one of the most important variables is the peel hue because it is used to
 383 determine fruit ripeness (Mendoza and Aguilera, 2004; OLIVEIRA et al., 2017). This is very important to
 384 plan harvesting procedures. In an experiment described in Oliveira et al. (2018), the hue component was
 385 measured for a sample of 20 papaya fruits using a flat-bed scanner (HP Scanjet G2410) and a colorimeter
 386 (Minolta CR-300) (Konica Minolta, 2003). The hue of each fruit was measured daily using both devices
 387 for a period of 15 days, where four equidistant points on the equatorial region were observed using a
 388 colorimeter, and 1,000 points over the same region were observed using a scanner. The circular mean
 389 hue was calculated for the i th fruit, $i = 1, 2, \dots, N$, measured by the j th method, $j = 1, 2$ at time t_{ik} ,
 390 $k = 1, 2, \dots, n_i$. As the multivariate von Mises distribution of the hue is highly concentrated around its
 391 overall mean, we assume that its distribution can be treated as a normal distribution with mean $\mu_{\bar{h}}$ and
 392 covariance matrix $\mathbf{R} = \mathbf{I}\sigma_{\varepsilon}^2$.

393 The aim of the agreement study here was to determine whether the scanner can reproduce the mean
 394 hue measurements taken by the colorimeter on the same fruit over time. The colorimeter is faster and
 395 easier to use than a flatbed scanner. Additionally, each image obtained with the scanner needs to be processed
 396 by an image manipulation program to select the object and extract its pixel-by-pixel information. Our
 397 major interest here is in the longitudinal accuracy profile, because high values over time would suggest
 398 that the fruit's topography does not influence the measurements taken by the scanner.

399 We start by making a plot of individual profiles grouped by measurement device, as well as a scatterplot
 400 of the hue data (Figure 3). We fit a second-degree polynomial model over time for each fruit considering
 401 all observations taken by both devices, and obtain the 95% confidence intervals for the coefficients (Figure
 402 3(c)). Apparently, there is a moderate agreement between the scanner and the colorimeter, which increases
 403 as the mean hue decreases. However, this could be due to the smaller number of fruits at the end of the
 404 experiment (fruits that presented disease had to be dropped out of the study).

405

406 Let y_{ijk} be the peel hue measured on fruit i , using method j at time point k . We start by fitting a second
 407 degree polynomial mixed-effects model with random intercepts, linear and quadratic coefficients, written
 408 as

$$y_{ijk} = \beta_{0j} + b_{0i} + (\beta_{1j} + b_{1i})t_k + (\beta_{2j} + b_{2i})t_k^2 + \varepsilon_{ijk},$$

$$\mathbf{b} = [b_{0i}, b_{1i}, b_{2i}]^T \sim N_3(\mathbf{0}, \mathbf{G}) \quad \text{and} \quad \varepsilon_{ijk} \sim N(0, \sigma_{\varepsilon}^2), \quad (5)$$

409 where $\text{vech}(\mathbf{G}) = [\sigma_{b_0}^2, \sigma_{b_{01}}, \sigma_{b_{02}}, \sigma_{b_1}^2, \sigma_{b_{12}}, \sigma_{b_2}^2]^T$. Under the model (5), the LCC is given by

$$\rho_{jj'}(t_k) = \frac{\mathbf{t}_k \mathbf{G} \mathbf{t}_k^T}{\mathbf{t}_k \mathbf{G} \mathbf{t}_k^T + \sigma_{\varepsilon}^2 + \frac{1}{2} S_{jj'}^2(t_k)}.$$

410 We can fit this model to estimate the LCC, LPC and LA statistics as well as to compute their 95% bootstrap
 411 confidence intervals based on 10,000 pseudo-samples using the `lcc()` function directly:

```
412 R> data(hue)
413 R> set.seed(6836)
414 R> m.hue.2 <- lcc(data = hue, subject = "Fruit", resp = "H_mean",
415 +               method = "Method", time = "Time", qf = 2, qr = 2,
416 +               ci = TRUE, nboot = 10000, components = TRUE)
417 Convergence error in 3133 out of 10000 bootstrap samples.
```

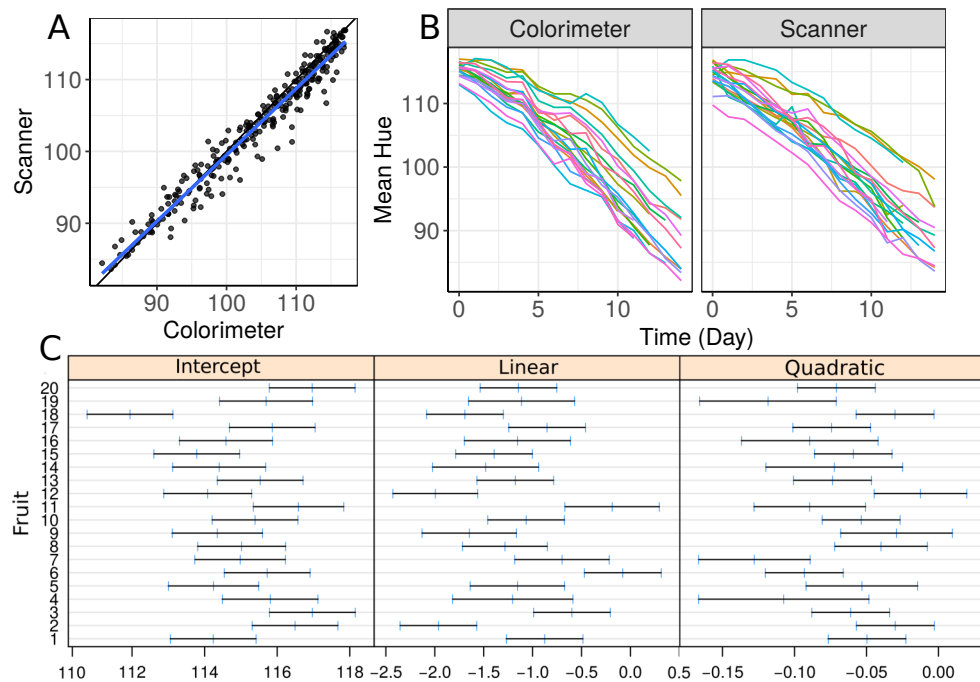


Figure 3. (A) Scatterplot of hue data considering all repeated measurements with a blue line representing the best fit line and the black one the line of equality, (B) Individual profiles of the peel hue of 20 papaya fruits measured by a colorimeter and a scanner, and (C) individual 95% confidence intervals for second degree polynomial coefficients fitted to the data on each fruit considering all methods together

418 The model used to estimate $\rho_{jj'}(t_k)$ as well as its sampled and fitted values can be extracted by
 419 using `summary(m.hue.2, type = "model")` and `summary(m.hue.2, type = "lcc")`,
 420 respectively. Moreover, a graphical representation of fitted values and confidence intervals for LCC, LPC
 421 and LA can be obtained by executing

```
422 R> lccPlot(m.hue.2)
423 R> lccPlot(m.hue.2, type = "lpc")
424 R> lccPlot(m.hue.2, type = "la")
```

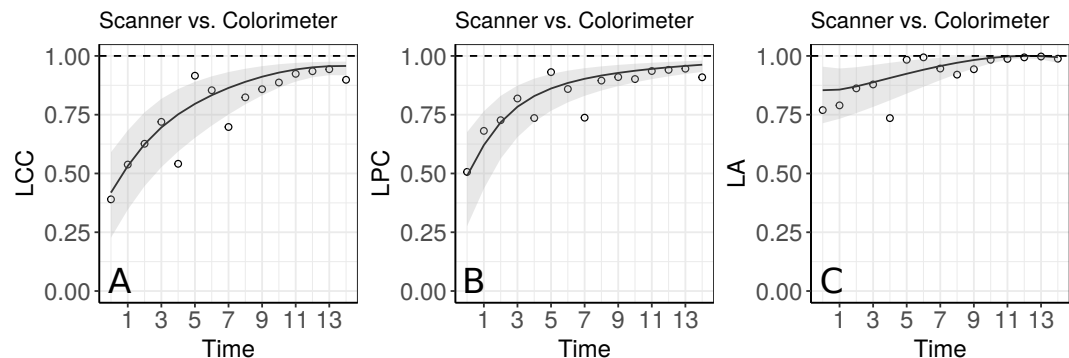


Figure 4. Estimate and 95% bootstrap confidence interval for the (A) longitudinal concordance correlation (LCC); (B) longitudinal Pearson correlation; and (C) longitudinal accuracy between observations measured by the scanner and the colorimeter with points that represent the (A) sample CCC, (B) sample Pearson correlation coefficient, and (C) sample accuracy, using model (5)

425 Apparently, the estimated LCC increases over time (Figure 4A). However, note that it is necessary to
 426 check whether the model assumptions were fulfilled because the estimates for the LCC and its bootstrap

427 confidence intervals may be biased under a misspecified model. We therefore checked (i) the normality
 428 assumption for the errors, by producing a normal plot of the within-group standardized residuals (Figure
 429 S1(a)), which indicates that this assumption for the within-group errors is almost plausible, and is not far
 430 from a normal distribution; ii) the homoscedasticity over time was evaluated via a plot of the standardized
 431 residuals versus time (Figure S1(b)), which indicates an apparent residual correlation for observations
 432 taken by the colorimeter and greater between-subject variance for observations taken by the scanner
 433 (Figure S2); iii) the normality assumption for the random effects (Figure S1(c)), which are verified by
 434 producing a normal plot for b_{0i} , b_{1i} and b_{2i} . Additionally, the goodness of fit (gof) was 0.992, indicating
 435 a high concordance among the model fitted values and observed values. Thus, we update the model
 436 `m.hue.2` to include different variances for each level of the factor "method", where the variance function
 437 is given by:

$$\text{Var}(\varepsilon_{ijk}) = \sigma_{\varepsilon}^2 \delta_j^2, \text{ with } j = 1, 2.$$

438 To ensure identifiability we assume that $\delta_1 = 1$. We also created a regular sequence from the time variable
 439 that can be used to make predictions

```
440 R> lcc_time <- with(hue, list(time = Time, from = min(Time),
441 +                           to = max(Time), n = 50))
```

442 This model can be specified in the `lcc()` as

```
443 R> set.seed(6836)
444 R> m.hue.3 <- update(m.hue.2, var.class = varIdent, weights.form = "method",
445 +                   time_lcc = lcc_time,
446 +                   lme.control = lmeControl(opt = "optim"))
447 Convergence error in 1187 out of 10000 bootstrap samples.
```

448 As models `m.hue.2` and `m.hue.3` are nested, we can use the likelihood ratio to test the hypothesis
 449 $H_0 : \delta_2^2 = 1$ versus $H_a : \delta_2^2 \neq 1$:

```
450 R> anova(m.hue.2, m.hue.3)
451 Model df      AIC      BIC      logLik      Test      L.Ratio      p-value
452 1     13  1938.125  1994.107  -956.0625
453 2     14  1934.920  1995.207  -953.4598  1 vs 2  5.205331  0.0225
```

454 The result shows that we reject H_0 in favour of H_a at a significance level of $\alpha = 0.05$, that is, the
 455 inclusion of the function $g(\delta_j) = \delta_j^2$ was significantly important in explaining the extra variability
 456 between observations taken at different times.

457 Moreover, the gof between fitted and observed values for `m.hue.3` model has, practically, the same
 458 value as presented for the `m.hue.2` model.

```
459 R> summary(m.hue.3, type = "lcc")$gof
460 [1] 0.9915905
```

461 Although the parameter δ_2^2 was important to explain the variability by method, we can see in Figure
 462 S3 that the model assumptions were still not completely fulfilled because there is a possible correlation
 463 among residuals for the colorimeter methodology. However, this model is more plausible than the first
 464 one. The sample semivariogram estimate is presented in Figure S3(b) and it appears to vary non-randomly
 465 around 0.9. Further studies involving the inclusion of correlation structures for the within-group residuals
 466 to compute the longitudinal concordance correlation function are still in development.

467 The agreement profile changes over time, being smaller at the beginning of the experiment and
 468 increasing to values close to 1 (Figure 5). If we consider values above 0.80 for the lower bound of the CI
 469 as an indication for interchangeability between the use of the two methods, the colorimeter could be used
 470 from the 12th day onwards.

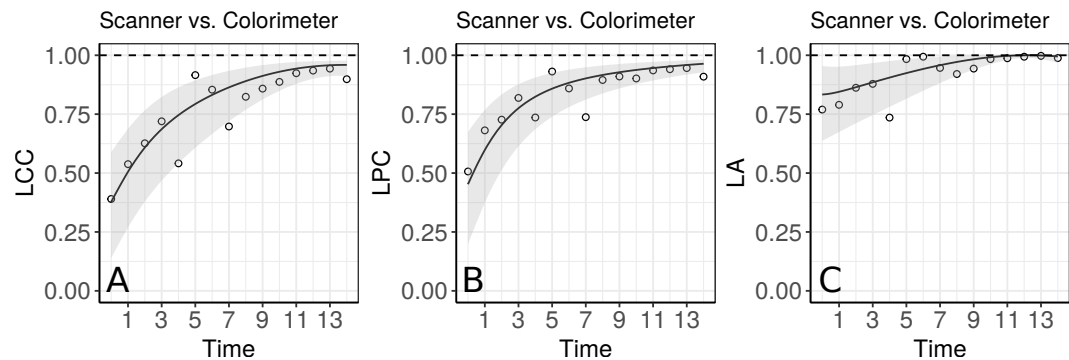


Figure 5. Estimate and 95% bootstrap confidence interval for the (A) longitudinal concordance correlation (LCC); (B) longitudinal Pearson correlation; and (C) longitudinal accuracy between observations measured by the scanner and the colorimeter with points that represent the (A) sample CCC, (B) sample Pearson correlation coefficient, and (C) sample accuracy, using the model that estimates different variances for each method

471 The blood draw dataset

472 The blood draw dataset was used as an example in the `cccrm` package developed by Carrasco et al. (2013).
 473 This dataset comes from a study conducted by the Asthma Clinical Research Network (ACRN) (Martin
 474 et al., 2002). In this double-blinded clinical trial, 144 subjects were randomized to one of six inhaled
 475 corticosteroid combinations, and the primary aim of the study was to estimate dose-response curves with
 476 respect to adrenal suppression. After two weeks, the subjects were admitted for overnight testing once a
 477 week, for the next five weeks (visits). Blood samples were collected hourly between 8pm and 8am. Then,
 478 the plasma cortisol area under the curve (AUC) was calculated using the trapezoidal rule. A secondary
 479 objective here was to assess the agreement of the results from blood sampling performed hourly or every
 480 two hours, when calculating the plasma cortisol AUC. As an example, we used all individual profiles
 481 whose expected value can be described using a second or lower degree polynomial mixed-effects model:

```

482 R> data(bdaw, package = "cccrm")
483 R> bdaw$SUBJ <- as.factor(bdaw$SUBJ)
484 R> bdaw$MET <- as.factor(bdaw$MET)
485 R> levels(bdaw$MET) <- c("1 hour", "2 hours")
486 R> length(unique(bdaw$SUBJ))
487 R> library(nlme)
488 R> fit_list <- lmList(AUC ~ poly(VNUM, 4) | SUBJ, data = bdaw)
489 R> int <- intervals(fit_list)
490 R> zero_included <- function(x) {
491 +   flag <- min(x) < 0 & max(x) > 0
492 +   return(flag)
493 + }
494 R> selected_subj <- names(
495 +   which(apply(int[, , 4], 1, zero_included) &
496 +     apply(int[, , 5], 1, zero_included)))
497 R> bdaw_subset <- subset(bdaw, SUBJ %in% selected_subj)

```

498 The scatterplot of the AUC taken every two hours as a function of the AUC taken each hour and plots of
 499 the 19 selected individual profiles are presented in Figure 6.

500 There seems to be a moderate to strong agreement between the plasma cortisol AUC measurements
 501 from blood draw samples taken hourly and every two hours (Figure 6A). Furthermore, we can also see
 502 high variability between subjects and that the AUC decreases over time for some subjects (Figure 6B).
 503 We begin by fitting a first degree polynomial model with a subject random intercept and slope model.

```

504 R> m.bw.1 <- lcc(data = bdaw_subset, subject = "SUBJ",
505 +               resp = "AUC", method = "MET", time = "VNUM",

```

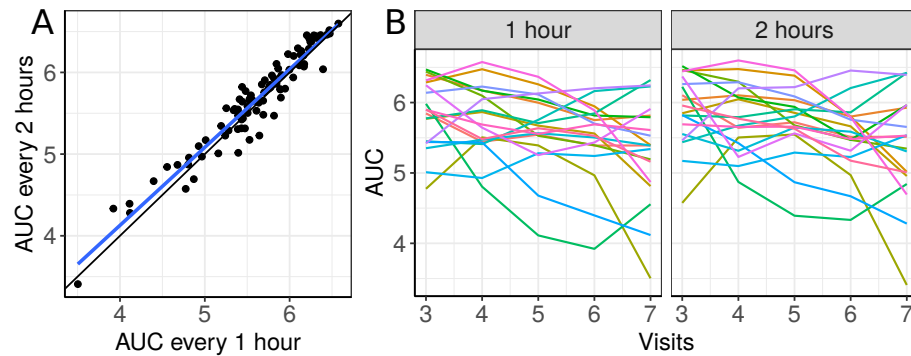


Figure 6. (A) Scatterplot of the blood draw data considering all repeated measurements (best fit line in blue and equality line in black), and (B) individual profiles of the plasma cortisol AUC calculated from measurements taken every hour and every two hours.

```

506 +               qf = 1, qr = 1)
507 R> summary(m.bw.1, type = "lcc")$gof
508 [1] 0.8850628

```

509 This model gives only a moderate fit to the data and this is confirmed by the estimated CCC between fitted
 510 and sampled values of 0.885 (Figure 7C). Two possible reasons are (i) we need a higher degree polynomial
 511 mixed model to correctly describe some subject profiles, and/or (ii) a possible heteroscedasticity across
 512 time, potentially caused by three somewhat different subject profiles, that should be included in the model
 513 (Figure 7B). In addition, the normality assumptions for the within group error and random effects were
 514 easily checked by producing the normal plot with simulation envelope (Figures 7E & F) and seem to be
 515 broadly plausible.

```

516 R> plot(m.bw.1, which = c(1, 2, 4, 5, 6))

```

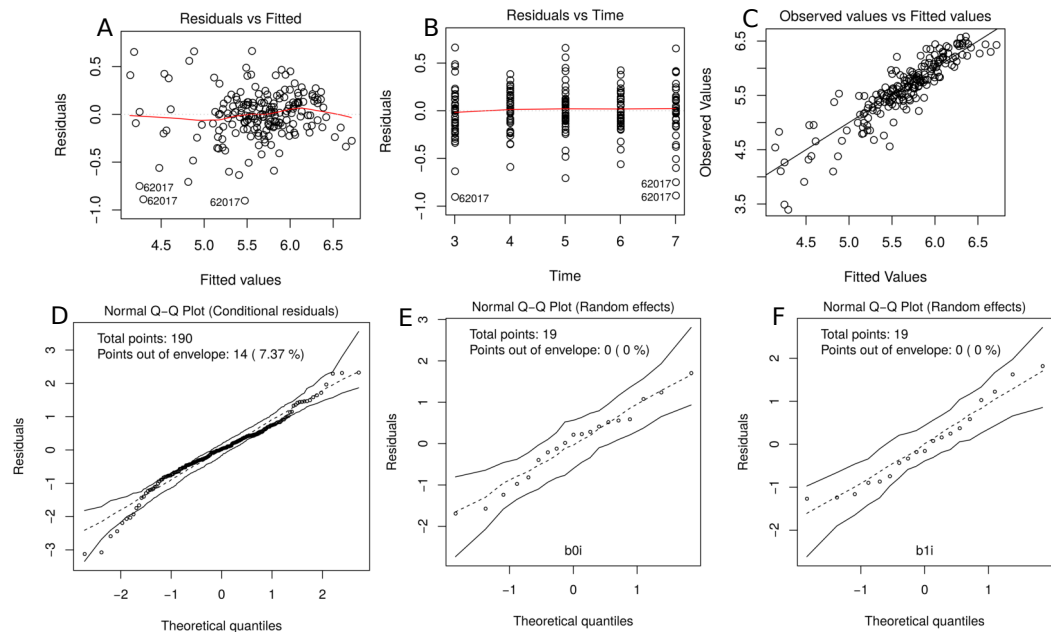


Figure 7. (A) plot of standardized residuals versus fitted values, (B) standardized residuals versus visits; (C) observed values versus fitted values; (D) Normal Q-Q plot with 95% simulation envelope for the conditional residuals; and (E and F) normal Q-Q plot with 95% simulation envelope for random effects

517 We now fit a second degree polynomial model with random subject effects for all coefficients and

518 compute the 95% bootstrap confidence intervals based on 10.000 bootstrap samples for LCC, LPC and
519 LA components.

```
520 R> m.bw.2 <- update(m.bw.1, qf = 2, qr = 2, components = TRUE,
521 +                   time_lcc = list(from = 3, to = 7, n = 50),
522 +                   ci = TRUE, nboot = 10000, show.warnings = TRUE,
523 +                   lme.control = lmeControl(msMaxIter = 200,
524 +                   msMaxEval = 600, maxIter = 200), numCore = 4)
525 Convergence error in 0 out of 10000 bootstrap samples.
```

526 The summary of the mixed effects model used to estimate LCC, LPC and LA is presented below:

```
527 R> summary(m.bw.2)
528 Linear mixed-effects model fit by REML
529 Data: Data
530 AIC          BIC          logLik
531 33.93831    75.73247   -3.969153
532
533 Random effects:
534 Formula: ~fmla.rand - 1 | subject
535 Structure: General positive-definite
536
537                               StdDev          Corr
538 fmla.rand(Intercept)          3.1753653 fm.(I) fd=qr=T
539 fmla.randpoly(time, degree = qr, raw = TRUE)1 1.3857944 -0.986
540 fmla.randpoly(time, degree = qr, raw = TRUE)2 0.1404521  0.961 -0.991
541 Residual                      0.1269293
542
543 Fixed effects: resp ~ fixed - 1
544
545                               Value Std.Error DF t-value p-value
546 fixed(Intercept)              6.0147  0.75167 166  8.0018  0.0000
547 fixedmethod2 hours              0.0471  0.26203 166  0.1796  0.8576
548 fixedPoly1                    -0.0277  0.32744 166 -0.0847  0.9326
549 fixedPoly2                    -0.0101  0.03315 166 -0.3046  0.7611
550 fixedmethod2 hours:Poly1       0.0107  0.11083 166  0.0967  0.9231
551 fixedmethod2 hours:Poly2      -0.0017  0.01101 166 -0.1500  0.8809
552
553 Correlation:
554
555                               fxd(I) fxdm2h fxdPl1 fxdPl2 f2h:P1
556 fixedmethod2 hours            -0.174
557 fixedPoly1                    -0.986  0.167
558 fixedPoly2                    0.961 -0.160 -0.991
559 fixedmethod2 hours:Poly1      0.172 -0.989 -0.169  0.165
560 fixedmethod2 hours:Poly2     -0.168  0.966  0.168 -0.166 -0.993
561
562 Standardized Within-Group Residuals:
563
564                               Min          Q1          Med          Q3          Max
565 -2.97645030 -0.48398412  0.03947773  0.59922913  1.87267383
566
567 Number of Observations: 190
568 Number of Groups: 19
```

Now we can test the hypotheses

$$H_0 : \sigma_{b_0}^2 > 0, \sigma_{b_1}^2 > 0, \sigma_{b_{12}} > 0, \sigma_{b_2}^2 = \sigma_{b_{02}} = \sigma_{b_{12}} = 0 \quad \text{vs.} \quad H_a : D \text{ is positive definite}$$

564 which is equivalent to testing whether the additional variance components of the model m.bw.2 in
565 relation to m.bw.1 are equal to zero:

```
566 R> m.bw.3 <- update(m.bw.1, qf = 2)
```

```

567 R> anova(m.bw.3, m.bw.2)
568           Model df   AIC      BIC   logLik Test L.Ratio p-value
569 m.bw.3      1    10 207.642 239.792 -93.821
570 m.bw.2      2    13  33.938  75.732  -3.969 1 vs 2  179.70 <.0001

```

571 and these results clearly show that those additional variance components are important. Furthermore,
 572 the CCC between fitted and observed values also indicates that model *m.bw.2* fits better than model
 573 *m.bw.1*, and *m.bw.3*.

```

574 R> summary(m.bw.1, type="lcc")$gof
575 [1] 0.8850628
576 R> summary(m.bw.2, type="lcc")$gof
577 [1] 0.9830078
578 R> summary(m.bw.3, type="lcc")$gof
579 [1] 0.8856218

```

580 Figure 5 shows the fitted LCC, LPC, and LA for concentration of plasma cortisol AUC between
 581 measurements taken every hour and taken every 2 hours and their respective 95% confidence intervals.

```

582 R> lccPlot(m.bw.2, control = list(scale_y_continuous = c(0.85, 1)))
583 R> lccPlot(m.bw.2, type = "lpc",
584 +         control = list(scale_y_continuous = c(0.85, 1)))
585 R> lccPlot(m.bw.2, type = "la",
586 +         control = list(scale_y_continuous = c(0.85, 1)))

```

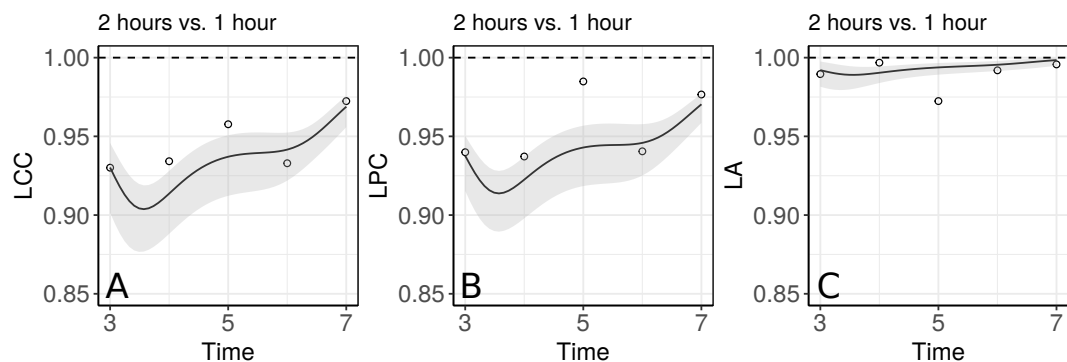


Figure 8. Estimate and 95% bootstrap confidence interval for (A) longitudinal concordance correlation (LCC); (B) longitudinal Pearson correlation; and (C) longitudinal accuracy for the plasma cortisol AUC between measurements taken every hour and taken every 2 hours. In addition, points that represent the sample CCC, sample Pearson correlation coefficient, and sample accuracy, respectively

587 These results show that even though the trend across time is essentially linear at the population level, there
 588 is a non-linear trend at the individual level to be more investigated. We can observe that the fitted values
 589 and confidence intervals for the LA component were very close to 1 over time, indicating a very high
 590 accuracy between methods (Figure 8C). Consequently, the LCC values depend almost exclusively on the
 591 LPC, which indicates a possible problem related to the precision between methods over time, suggesting
 592 the use of blood sampled every hour, rather than every two hours, is desirable for this group of patients.
 593 It is worthy to note that, as the diagnostic seems broadly plausible for the second degree mixed effects
 594 polynomial model (*m.bw.2*), under this model the LCC, LPC, and LA are fourth degree polynomials
 595 functions of the time variable.

596 Additionally, as the `lcc()` function includes the interaction between time and method as default
 597 through the argument `interaction = TRUE`, we can test if the interaction effect is necessary using,
 598 for example, the following code:

```

599 R> m.bw.4 <- lcc(data = bdaw_subset, subject = "SUBJ",
600 +             resp = "AUC", method = "MET", time = "VNUM",

```

```

601 +           qf = 2, qr = 2, REML = FALSE, interaction = FALSE)
602 R> m.bw.5 <- update(m.bw.4, interaction = TRUE)
603 R> anova(m.bw.4, fit.bw5)
604           Model df   AIC   BIC   logLik   Test   L.Ratio p-value
605 m.bw.4       1    11 -2.5416 33.176  12.271
606 m.bw.5       2    13  1.2332 43.445  12.383  1 vs 2  0.22520  0.8935

```

607 The large p-value (0.8935) obtained from the likelihood ratio test, as well as the lower AIC and BIC values
608 obtained for model (4) when compared to model (5), suggests no evidence that a model with different
609 slopes describes the data significantly better. Therefore, we opt for the reduced model (4) to analyse
610 the blood draw data. Thus, all of these examples show that our methodology is very flexible and can be
611 applied to many different data types, but the user should be careful about avoiding overfitting. We have
612 also created a Shiny app (<https://prof-thiagooliveira.shinyapps.io/lccApp/>) using simulated data in order
613 to stimulate people to learn more about the LCC and verify how each parameter's value can affect the
614 estimation of the LCC, LPC, and LA.

615 DISCUSSION

616 The package `lcc` provides a convenient and versatile tool for estimation and inference about the LCC,
617 LPC, and LA. The estimation of these three statistics provides a complete evaluation of the agreement
618 between methods over time (Oliveira et al., 2018). These statistics are also very appealing for graphical
619 illustration.

620 The package supports balanced or unbalanced (dropouts) experimental designs or observational
621 studies, multiple methods, inclusion of covariates in the linear predictor to control systematic variation in
622 the response, and the inclusion of different variance-covariance structures for random-effects and residuals.
623 Residual diagnostic and goodness of fit can be evaluated easily via the generic function `plot()`, which
624 provides up to six built-in diagnostic plots. Furthermore, the `anova()`, `AIC()`, and/or `BIC()` functions
625 can be used to aid in model selection.

626 Statistical inference for the estimators of $\rho_{jj'}(t_k)$, $\rho_{jj'}^{(p)}(t_k)$, and $C_{jj'}(t_k)$ can be obtained using bootstrap
627 confidence intervals based on approximations of their empirical distributions by the normal distribution,
628 or from percentiles of their bootstrap sampling distribution. These methods are, however, computationally
629 intensive.

630 To the best of our knowledge, there is no package available to estimate the extent of longitudinal
631 agreement between methods. The `lcc` package can be viewed as an extension of the R and SAS `ccorm`
632 package developed by Carrasco et al. (2013). This package handles the time as a factor in the model, and
633 computes the concordance correlation coefficient, which can be viewed as a measure that summarises the
634 interchangeability between methods in relation to all their measurements.

635 The importance in estimating the LPC, as a measure of precision, and the LA, as a measure of
636 accuracy, was demonstrated in Section (Figure 5). In particular, both of these statistics can be used jointly
637 to determine if a moderate or small agreement between methods at time $t_k = t$ is related to a precision
638 or an accuracy problem, as suggested by Lin (1989); Barnhart and Williamson (2001); Lin (1992); Ma
639 et al. (2010). In the papaya hue example, the moderate LCC is highly influenced by a moderate LPC,
640 suggesting that if we increase the number of points observed with the colorimeter on the equatorial region
641 up to day 10, the colorimeter will probably be able to reproduce the measurements taken by the scanner.
642 Future studies involve the determination of the sample size over time based on the least acceptable LCC,
643 assuming we can accept up to a certain amount of loss in the LPC and in the LA, as discussed by Lin
644 (1992).

645 It would be useful to mention that, as a naive analysis, the Bland-Altman method (Bland and Altman,
646 1986) is commonly used to calculate the mean difference between two methods (as a measurement of
647 "bias") with the addition of 95% limits of agreement (LoA) in the analysis of repeated-measures studies
648 (including longitudinal data). If these methods are being compared without a 'golden standard' reference
649 (Lin, 1989), an improved Bland-Altman interval approach is preferred (Liao and Capen, 2011).

650 Although these approaches are not suitable to analyse repeated-measures designs, researchers still use
651 it to explore the data because the method is simple to use. However, even if the Bland-Altman method has
652 observations outside of LoA range, two methods can have a very high concordance correlation when the
653 correct variance-covariance structure is accounted for in the model, as discussed by Zhao et al. (2009).

654 This demonstrates the value of the availability of packages that enable the selection of matrix structures
655 for random effects and error term when calculating the longitudinal concordance correlation.

656 Another interesting remark is that when the systematic difference between methods is zero, the
657 CCC calculated based on a mixed-effects model is equivalent to the intraclass correlation coefficient
658 (ICC) (Carrasco et al., 2009). In the same direction, the ICC as a function of the time variable is a
659 particular case of the longitudinal concordance correlation function when $S_{jj}^2(t_k) = 0$. If we consider the
660 repeated measures, the ICC gives us the percentage of total variability explained by subject over time,
661 and, consequently, it is not comparable with the LCC in terms of a longitudinal agreement index between
662 methods.

663 Finally, all examples discussed in Section show that our methodology is flexible, and can be applied
664 to many different data types. One limitation of the `lcc` package is that, for the time being, the `covar`
665 argument only allows for including fixed-effect covariates in the linear predictor. We plan to update our
666 package in the near future to handle with the inclusion of fixed-effects and random-effects covariates, as
667 well as interaction effects.

668 CONCLUSION

669 The `lcc` package implements methods to estimate the LCC, LPC and LA functions as well as their
670 bootstrap confidence intervals. In this package, we included different structures for the variance-covariance
671 matrices of random-effects and residuals, allowing estimation of the extent of longitudinal agreement
672 between methods under different assumptions. Functions `plot()`, for diagnostics, `summary()` and
673 `lccPlot()`, for numerical and graphical summaries, respectively, and `anova()`, `AIC()`, `BIC()`, for
674 model selection, make the package flexible and easy to use. Furthermore, the mixed-effects model based
675 approach to compute the LCC allows us to work with both balanced and unbalanced experimental designs
676 and observational studies.

677 ACKNOWLEDGEMENTS

678 The authors are grateful to CNPq (National Council of Technological and Scientific Development),
679 CAPES (Coordination for the Improvement of Higher Education Personnel), University of São Paulo, and
680 National University of Ireland Galway, that supported this research project. We extend our thanks for
681 the Science Foundation Ireland (SFI) under grant number SFI/12/RC/2289, co-funded by the European
682 Regional Development Fund. This manuscript benefited from insightful comments and suggestions
683 provided by two anonymous reviewers and an academic editor.

684 REFERENCES

- 685 Akaike, H. (1974). A New Look at the Statistical Model Identification. *IEEE Transactions on Automatic*
686 *Control*, 19(6):716–723.
- 687 Auguie, B. and Antonov, A. (2017). `gridExtra`: Miscellaneous Functions for ‘Grid’ Graphics.
- 688 Barnhart, H. X. and Williamson, J. M. (2001). Modeling concordance correlation via GEE to evaluate
689 reproducibility. *Biometrics*, 57(3):931–940.
- 690 Bland, J. M. and Altman, D. G. (1986). Statistical methods for assessing agreement between two methods
691 of clinical measurement. *The Lancet*, 1(8476):307–310.
- 692 Carrasco, J. L., King, T. S., and Chinchilli, V. M. (2009). The concordance correlation coefficient
693 for repeated measures estimated by variance components. *Journal of biopharmaceutical statistics*,
694 19(1):90–105.
- 695 Carrasco, J. L., Phillips, B. R., Puig-Martinez, J., King, T. S., and Chinchilli, V. M. (2013). Estimation of
696 the concordance correlation coefficient for repeated measures using SAS and R. *Computer Methods*
697 *and Programs in Biomedicine*, 109:293–304.
- 698 Chen, C. C. and Barnhart, H. X. (2013). Assessing agreement with intraclass correlation coefficient and
699 concordance correlation coefficient for data with repeated measures. *Computational Statistics and*
700 *Data Analysis*, 60(1):132–145.
- 701 Chinchilli, V. M., Martel, J. K., Kumanyika, S., and Lloyd, T. (1996). A Weighted Concordance
702 Correlation Coefficient for Repeated Measurement Designs. *Biometrics*, 52(1):341–353.

- 703 Giesbrecht, F. G. and Burns, J. C. (1985). Two-Stage Analysis Based on a Mixed Model: Large-Sample
704 Asymptotic Theory and Small-Sample Simulation Results. *International Biometric Society*, 41(2):477–
705 486.
- 706 Harville, D. A. (1977). Maximum Likelihood Approaches to Variance Component Estimation and to
707 Related Problems. *Journal of the American Statistical Association*, 72(358):320–338.
- 708 King, T. S. and Chinchilli, V. M. (2001). A generalized concordance correlation coefficient for continuous
709 and categorical data. *Statistics in Medicine*, 20(14):2131–2147.
- 710 King, T. S., Chinchilli, V. M., Wang, K.-L., and Carrasco, J. L. (2007). A class of repeated measures
711 concordance correlation coefficients. *Journal of biopharmaceutical statistics*, 17:653–672.
- 712 Konica Minolta (2003). *Precise colour communication, colour control from perception to instrumentation*.
713 Konica Minolta Sensing.
- 714 Liao, J. J. (2005). Agreement for curved data. *Journal of Biopharmaceutical Statistics*, 15(2):195–203.
- 715 Liao, J. J. and Capen, R. (2011). An improved bland-altman method for concordance assessment.
716 *International Journal of Biostatistics*, 7(1).
- 717 Liao, J. J. Z. (2003). An improved concordance correlation coefficient. *Pharmaceutical Statistics*,
718 2(4):253–261.
- 719 Lin, L. I. (1989). A Concordance Correlation Coefficient to Evaluate Reproducibility. *Biometrics*,
720 45(1):255–268.
- 721 Lin, L. I.-K. (1992). Assay Validation Using the Concordance Correlation Coefficient. *Biometrics*,
722 48(2):599.
- 723 Lloyd, T., Chinchilli, V. M., Egli, D. F., Rollings, N., and Kulin, H. E. (1998). Body composition
724 development of adolescent white females. *Archives of Pediatric Adolescence Medicine*, 152:998—
725 1002.
- 726 Loecher, M., Magrath, P., Aliotta, E., and Ennis, D. B. (2019). Time-optimized 4D phase contrast MRI
727 with real-time convex optimization of gradient waveforms and fast excitation methods. *Magnetic
728 Resonance in Medicine*, 82(1):213–224.
- 729 Ma, Y., Tang, W., Yu, Q., and Tu, X. M. (2010). Modeling concordance correlation coefficient for
730 longitudinal study data. *Psychometrika*, 75(1):99–119.
- 731 Martin, R. J., Szefer, S. J., Chinchilli, V. M., Kraft, M., Dolovich, M., Boushey, H. A., Cherniack, R. M.,
732 Craig, T. J., Drazen, J. M., Fagan, J. K., Fahy, J. V., Fish, J. E., Ford, J. G., Israel, E., Kunselman, S. J.,
733 Lazarus, S. C., Lemanske, R. F., Peters, S. P., and Sorkness, C. A. (2002). Systemic effect comparisons
734 of six inhaled corticosteroid preparations. *American Journal of Respiratory and Critical Care Medicine*,
735 165(10):1377–1383.
- 736 Mendoza, F. and Aguilera, J. M. (2004). Application of image analysis for classification of ripening
737 bananas. *Journal of food science*, 69(9):471–477.
- 738 Moral, R. A., Hinde, J., and Demétrio, C. G. (2017). Half-normal plots and overdispersed models in R:
739 The hnp package. *Journal of Statistical Software*, 81(10).
- 740 Oliveira, T. d. P., Hinde, J., and Zocchi, S. S. (2018). Longitudinal concordance correlation function based
741 on variance components: an application in fruit color analysis. *Journal of Agricultural, Biological, and
742 Environmental Statistics*, 23(2):233–254.
- 743 OLIVEIRA, T. D. P., ZOCCHI, S. S., and JACOMINO, A. P. (2017). MEASURING COLOR HUE IN
744 ‘SUNRISE SOLO’ PAPAYA USING A FLATBED SCANNER. *Revista Brasileira de Fruticultura*,
745 39(2).
- 746 Oliveira, T. P., Moral, R. A., Hinde, J., Zocchi, S. S., and Demétrio, C. G. B. (2019). Longitudinal
747 Concordance Correlation.
- 748 Pandit, V., Chair, Z. B., and Schuller, B. (2019). On Many-to-Many Mapping Between Concordance
749 Correlation Coefficient and Mean Square Error. *arXiv*, pages 1–24.
- 750 Pinheiro, J., Bates, D., Debroy, S., Sarkar, D., and core team, R. (2017). nlme: linear and nonlinear mixed
751 effects models.
- 752 Pinheiro, J. C. and Bates, D. M. (2000). *Mixed-Effects Models in S and S-PLUS*. Springer, New York.
- 753 R core Team (2019). The R environment.
- 754 Rathnayake, L. N. and Choudhary, P. K. (2017). Semiparametric modeling and analysis of longitudinal
755 method comparison data. *Statistics in Medicine*, 36(13):2003–2015.
- 756 Schwarz, G. (1978). Estimating the dimension of a model. In *Annals of Statistics*, pages 461–464.
- 757 Shinar, S., Berger, H., De Souza, L. R., and Ray, J. G. (2019). Difference in Visceral Adipose Tissue in

- 758 Pregnancy and Postpartum and Related Changes in Maternal Insulin Resistance. *Journal of Ultrasound*
759 *in Medicine*, 38(3):667–673.
- 760 Warnes, G. R., Bolker, B., Gorjanc, G., Grothendieck, G., Korosec, A., Lumley, T., MacQueen, D.,
761 Magnusson, A., and Rogers, J. (2017). *gdata: Various R Programming Tools for Data Manipulation*.
762 Wickham, H. (2009). *ggplot2: Elegant Graphics for Data Analysis*. New York.
- 763 Zhao, B., James, L. P., Moskowitz, C. S., Guo, P., Ginsberg, M. S., Lefkowitz, R. A., Qin, Y., Riely, G. J.,
764 Kris, M. G., and Schwartz, L. H. (2009). Evaluating variability in tumor measurements from same-day
765 repeat CT scans of patients with non-small cell lung cancer. *Radiology*, 252(1):263–272.